Investigation on Complex Permeability Spectra of Polycrystalline Li-Cd Ferrites

S. Karimunnesa*, D.P. Paul, S. Akhter, S. Akter[1] and D.K. Saha[2]

Department of Physics, University of Chittagong, Chittagong, Bangladesh
[1]Materials Science Division, Atomic Energy Centre, Dhaka, Bangladesh
[2]Planning and Development Division, Bangladesh Atomic Energy Commission, Agargaon, Dhaka

Abstract

Li-Cd ferrites of composition $Li_{0.5-x/2}Cd_xBi_{0.02}Fe_{2.48-x/2}O_4$ were prepared by double sintering ceramic technique at 970^0C and 1000^0C for 4 hours. Structural and magnetic properties of the Li-Cd ferrites were investigated. X-ray analysis indicated the single-phase cubic spinel structure for all samples. The lattice parameter was found to increase with increasing Cd content obeying Vegard's law. The X-ray density and bulk densities of the Li-Cd ferrite significantly increased whereas porosity decreased with increasing Cd concentration. Real part of initial permeability μ', Curie temperature T_c, imaginary part of the initial permeability μ", relative quality factor (Q-factor) of the samples were elaborately discussed as a function of frequency and temperature with increase of Cd content during the heating and cooling cycles. From temperature dependence permeability μ' at $T=T_c$, indicates that the samples have high homogeneity. The Curie temperature, T_c is found to decrease with increasing Cd content. The sample with x= 0.7 shows anomalous temperature dependent magnetic ordering. The initial permeability, μ' and magnetic loss factor, tanδ have been investigated up to 13 MHz frequency range. Frequency dependent permeability increases with increasing Cd content up to x = 0.6. The magnetic loss factor is minimum at frequency around 1 MHz and rises sharply beyond that frequency. The possible reasons responsible for change in structural and complex permeability with increasing of non-magnetic Cd^{2+} ion are ascertained.

Keywords: Ferrites, density, porosity, initial permeability, complex permeability, relative quality factor

1. Introduction

Polycrystalline soft ferrites prepared from metal oxides are magnetic semiconductors and have made important contribution in both technological and conceptual development of electronics and electronic industries. Up until today, soft ferrites remain the best magnetic materials which are irreplaceable by any other magnetic materials with respect to their very high frequency applications because they are inexpensive, more stable, easily manufactured [1]. They have wide variety of technological applications in transformer cores, inductors, high quality filters, radio frequency circuits, rod antennas, read/write heads for high-speed digital tape and operating devices as well [2-4]. Properties of soft ferrites are highly sensitive to preparation method, sintering conditions, amount of constituent metal oxides, various additives including dopants and impurities [5-8]. Among soft ferrites, Ni-Zn, Mg-Zn and Mn-Zn ferrites with various additives have enormous technological applications and accordingly extensive research have been carried out by many groups around the globe [9-13].

There are many experimental and theoretical investigations on the structural and frequency dispersion of complex permeability in polycrystalline ferrites [14-17]. The complex permeability spectra of polycrystalline ferrites depend not only on the chemical composition of the ferrite but also on the post-sintering density and the microstructure such as grain size and porosity. It was found that the sintering temperature has a great effect on the structural and magnetic properties of ferrites. In the present work, the influence of Cd on Li-Cd ferrites has been investigated by studying XRD and frequency dependence of complex permeability.

*Coorresponding author : syeda.karimunnesa45@gmail.com

2. Materials and Methods

The sample of stoichiometric composition $Li_{0.5-x/2}Cd_xBi_{0.02}Fe_{2.48-x/2}O_4$ (for x = 0.0, 0.1, 0.2, 0.3, 0.4, 0.5, 0.6 and 0.7) was prepared by conventional ceramic technique. Small amount of Bi_2O_3 (melting point 825ºC) was added to increase the densification at lower sintering temperature to minimize Li volatization during sintering as well as to improve magnetic and transport properties. Pure oxide powder of Li_2O, Fe_2O_3, CdO and Bi_2O_3 were weighed precisely according to their molecular weight. Intimate mixing of the materials was carried out using agate mortar for 4 h and then ball milled in a planetary ball mill in ethyl alcohol media for 2 h with stainless steel balls of different diameters. The slurry was dried and the dried power was pressed into disc shape. The disc shaped sample was pre-sintered at 850ºC for 10 h and then cooled to room temperature. The pre-sintered powders were again grounded thoroughly and then applying a pressure of 2 ton/cm^2, pellets were made of 1.34 cm diameter and 0.69 cm thick, toroids of 1.2 cm outer diameter and 0.6 cm inner diameter. Final sintering of the samples was carried out at 950ºC and 1000ºC for 4 hours to avoid the loss of lithium.

A PHILIPS PW3040 X'Pert PRO X-ray diffractometer (XRD) was used to get X-ray data at Materials Science Division, Atomic Energy Centre, Dhaka, Bangladesh. The powder diffraction technique was used with primary beam power of 40 kV and 30 mA for CuKα radiation. An HOPG secondary monochromator is used to remove CuKβ radiation and CuKα radiation as the primary beam. A θ - 2θ scan was taken from 20^0 to 70^0 to get possible fundamental peaks. The XRD machine was totally computer controlled and all the data were stored in hard disk memory of the computer for further analysis using computer software. The computer software, X'Pert High score, was used for phase identification. The initial magnetic permeability, μ'

calculated from the inductance values by an Inductance Analyzer, (WAYNE KERR, model 3255B) at room temperature on coil wound toroidal samples with an ac driving field of ~ 10^{-3}Oe up to 500 kHz. The sample was kept in a tubular furnace, which had good thermal insulation. The initial permeability was calculated using the relation $\mu' = L/L_0$, where L is the measured sample inductance and L_0 is the air core inductance using same dimensions of the toroid. The Curie temperature of the samples was determined from the temperature dependence of permeability. The frequency characteristics of the Li-Cd ferrite samples i.e. initial permeability spectra were investigated using Impedance Analyzer (Hewlett Packed model no. 4192A). The Complex permeability spectra of the toroid shaped samples were carried out at room temperature on all samples in the frequency range 1 kHz-13 MHz.

3. Results and Discussion

3.1 Structural Analysis

The structural study is essential for optimizing the properties needed for various applications. A typical XRD pattern indicating (hkl) values of each peaks corresponding to the sample x = 0.1 of $Li_{0.5-x/2}Cd_xBi_{0.02}Fe_{2.48-x/2}O_4$ ferrites is shown in Fig. 1. The XRD pattern of the sample, showing well-defined reflection without any ambiguity, exhibits the formation of single phase cubic spinel structure. Using XRD data, the lattice constant was determined by the Nelson-Riley extrapolation method [18]. The variation of the lattice constant *a* as a function of Cd content is found to increase linearly with increasing Cd content [19] obeying Vegard's law [11]. This increase in the lattice constant could be attributed to the ionic size difference as substituting by large ionic size Cd^{2+} (0.97 Å) [20] with that of Fe^{3+} ions (0.645 Å) [21]. The Results are in good agreement with the literature values of 8.34 Å [22] for Li-ferrite and 8.7Å for Cd-ferrites [23]. A similar linear variation has been observed in Zn-Mg, Li-Cd, Cd-Zn and Li-Mg ferrites [24-25].

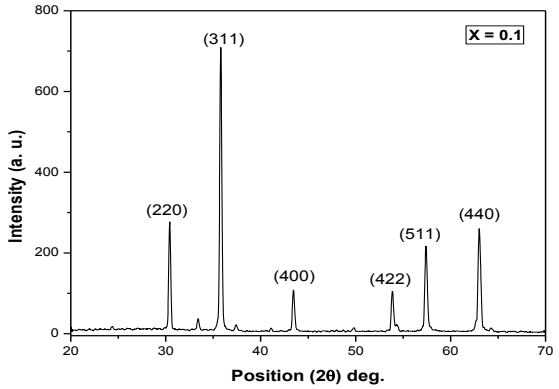

Fig. 1. XRD patterns of Cd doped Li-Cd ferrites

The X-ray or theoretical density and bulk density increases linearly with the increase of Cd concentration [19]. The result signifies that Cd has a pronounced effect on the densification of the Li-ferrites when it is substituted by cadmium. The highest density 5.73 g/cc is obtained for the composition of x=0.7. The increase in density with Mn substitution in Mg-Cu-Zn ferrites has also been reported [26]. The highest porosity is 12.13% at x=0.0, as demonstrates which further indicates that Cd has the beneficial effect on the densification of Cd substituted Li ferrites. The composition x=0.7 has the highest density and lowest porosity, as presented in Table 1.

Table 1. Experimental results of $Li_{0.5-x/2}Cd_xBi_{0.02}Fe_{2.48-x/2}O_4$ ferrites.

Cd content, x	Lattice parameter, a (Å)	Theoretical/x-ray density g/c.c.	Bulk density g/c.c.	Porosity (%)	Curie temperature, T_c(ºC)	Real part of permeabilit, μ'(1MHz) T_S = 970ºC	Real part of permeability, μ'(1MHz) T_S = 1000ºC
0.0	8.3303	5.11	4.49	12.13	670	45.34	48.29
0.1	8.3544	5.23	4.7	10.13	570	66.66	74.69
0.2	8.4069	5.3	4.74	10.57	473	83.81	90.68
0.3	8.4405	5.4	4.78	11.48	383	108.93	112.32
0.4	8.4701	5.53	4.93	10.85	295	118.56	119.32
0.5	8.505	5.62	4.97	11.57	205	123.78	125.73
0.6	8.5485	5.66	5.05	10.78	103	125.34	130.1
0.7	8.5926	5.73	5.22	8.90	-2	31.34	57.48

3.2 Temperature Dependence of Initial Permeability

Fig. 2 shows the thermal variation of initial permeability, μ' for x = 0.0 to 0.6. It is seen that μ' gradually increases with temperature reaching a maximum value and then drop sharply toward zero near the Curie temperature. The sharp decrease near Curie temperature suggests single-phase formation of the ferrites. This observation is supported by XRD studies, which do not show any impurity peaks.

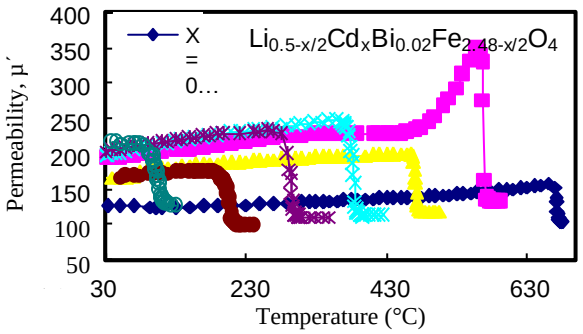

Fig. 2. Variation of initial permeability with temperature.

The compositional variation of μ' can be explained on the basis of Globus model [27]. According to this model μ' is given by

$$\mu' = (M_s^2 dm) / K_1 \quad (1)$$

Where M_s is the saturation magnetization, *dm* is average grain diameter and K_1 is magneto-crystalline anisotropy constant. Addition of Cd^{2+} to Li-ferrite initially increases M_s, dm and reduces K_1. The anisotropy constant and saturation magnetization usually decreases with increase in temperature, due to thermal agitation, which disturbs the alignment of magnetic moment. However, decrease of anisotropy constant with temperature is much faster than the decrease of M_s. When the anisotropy constant reaches zero, μ' attains its maximum value and then drops off to very low value. Thus, the effect of K_1 appears to be more significant in controlling the μ' of the ferrites materials. Similar results have been reported by Bellad et al. [23, 28] in the case of Li-Cd ferrites and also Shaikh et al. [29] in Li-Mg ferrites.

3.3 Frequency Dependence of Complex Permeability

Figs. 3(a), 4(a) and 3(b), 4(b) show the frequency dependence real and imaginary parts of permeability spectra of $Li_{0.5-x/2}Cd_xBi_{0.02}Fe_{2.48-x/2}O_4$ samples sintered at 970^0C and 1000^0C, respectively. It is clearly evident from Figs. 3(a) and 4(a) that with the increasing of Cd content x, the permeability μ' increases monotonically expect for x = 0.7. The sample with x = 0.7 is paramagnetic at room temperature. The real part of initial permeability μ' remains almost constant for x = 0.0 up to 13 MHz while for x = 0.1 and 0.2 it is almost stable up to 10 MHz. Again for sample x = 0.3-0.6, it is stable up to x = 5-7 MHz and then slightly decrease at higher frequency. Similar pattern is observed in Li-Zn ferrites by T. Nakamura [30]. Monotonic increase in grain size according to Globus [27] as well as increase in sintered density. The increase of μ' with the increase of Cd content results in a shift of the resonance frequency to lower frequency range according to Snoek's [31] relation, μf_r = constant, where f_r is the resonance frequency. Dispersion or resonance could not be observed with lesser content of Cd and lower sintering temperatures, since our measurement facility could not be extended beyond 15 MHz. Again this increasing permeability with increasing Cd content is connected with increased density, larger grain size and possibly reduction of anisotropy energy.

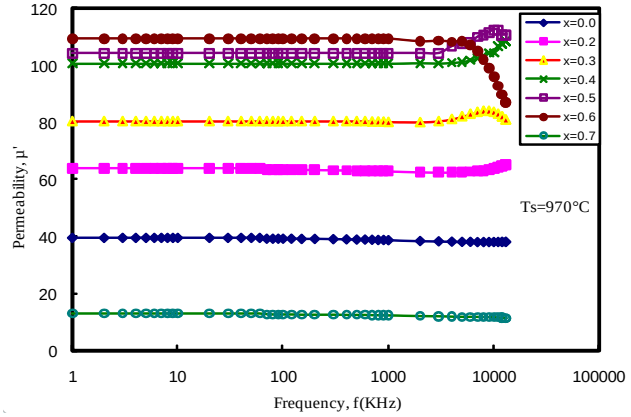

Fig. 3 (a). Real part of initial permeability (μ') vs frequency sintered at 970 ^{o} C for 4 hours.

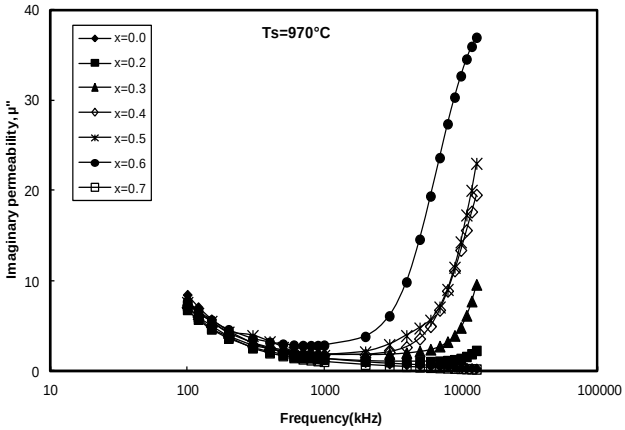

Fig. 3 (b). Imaginary part of initial permeability (μ") vs Frequency sintered at 970°C for 4 hours.

Figs. 3(b) and 4(b) represent the imaginary part of initial permeability, μ'' (loss component) of the samples sintered at 970^0C and 1000^0C respectively. It is observed from the figures that μ'' increases with increasing frequency and takes a broad maximum at a certain frequency. This feature is well known as the natural resonance. At the natural resonance, the imaginary permeability had a maximum value, shifted toward high frequency. The magnetic loss factor increased as the square of the frequency. Highest value of loss component of the complex permeability was observed for x=0.6. The same result is observed for Ni-Zn ferrite by Mahmud et al. [32].

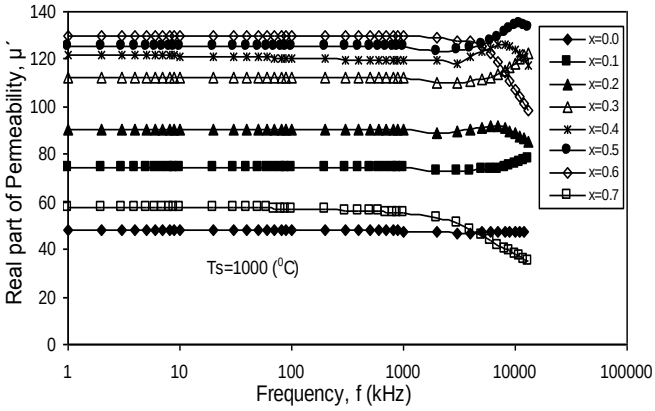

Fig. 4 (a). Real part of initial permeability (μ') vs frequency sintered at 1000°C for 4 hours.

3.4 Frequency Dependence of Relative Quality Factory (RQF)

Figs. 5(a) and 5(b) show the frequency dependence of relative quality factor (RQF) of the samples sintered at 970^0C and 1000^0C. The variation of the relative quality factor with frequency shows a similar trend for all the samples. Q-factor increases with an increase of frequency showing a peak and then decreases with further increase of frequency. It is seen that RQF decreases beyond 10MHz

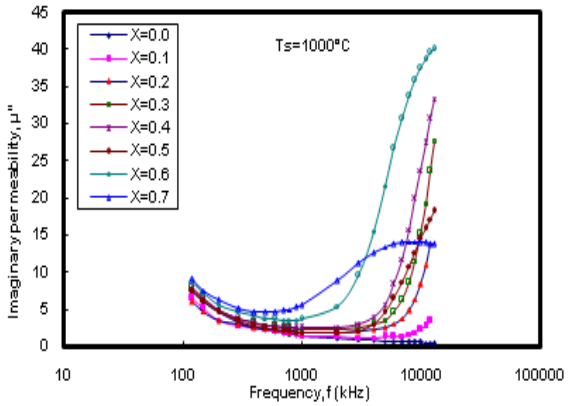

Fig. 4 (b). Imaginary part of initial permeability (μ") vs Frequency sintered at 1000°C for 4 hours.

i.e., the loss tangent is minimum up to 10 MHz and then it rises rapidly. The loss is due to log of domain wall motion with respect to the applied altering magnetic field and is attributed to various domain defects [33], which include non-uniform and non-repetitive domain wall motion, domain wall bowing, localized variation of flux density, and nucleation and annihilation of domain walls. This happens at the frequency where the permeability begins to drop with frequency. This phenomenon is associated with the ferromagnetic resonance within the domains [34] and at the resonance maximum energy is transferred from the applied magnetic field to the lattice resulting in the rapid decrease in RQF.

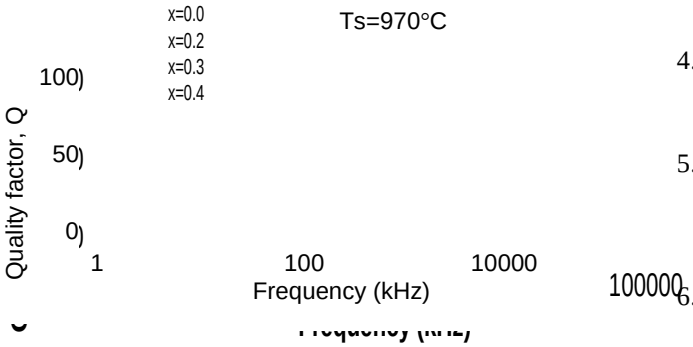

Fig. 5 (a). Quality Factor vs Frequency of the samples sintered at 970°C for 4hours.

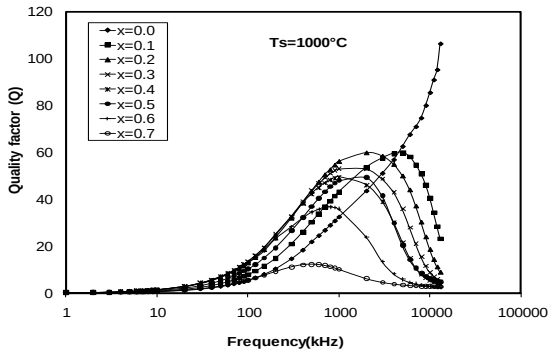

Fig. 5 (b). Quality Factor vs Frequency of the samples sintered at 1000°C for 4 hours.

4. Conclusions

The X-ray diffraction confirmed the single-phase cubic spinel structure of the samples. Initial permeability increases continuously with increase of Cd content as well as sintering temperature. The sharp fall of permeability at Curie temperature indicates that the samples have high homogeneity according to Globus. A linear decrease of Curie temperature with Cd content has been obtained and this is attributed to the weakening of J_{AB} exchange interaction. Initial permeability increases continuously with increase of Cd content as well as sintering temperature. Again this increasing permeability with increasing Cd content is connected with increased density, grain size and reduction of anisotropy energy with the addition of nonmagnetic Cd. Loss factor is minimum at around 1MHz frequency and rises sharply after 1 MHz can be associated with resonance phenomenon occurring in the domains passing through a maximum at a frequency known as resonance frequency.

References

1. J. Kulikowski, Soft Magnetic Ferrites-Development or Stagnation, J. Magn. Magn. Mater., **41**, 56 (1985).
2. A. Verma, T.C. Goel, R.G. Mendiratta and R.G. Gupta, High-Resistivity Nickel–Zinc Ferrites by the Citrate Precursor Method,. J. Magn. Magn. Mater., **192**, 271 (1999).
3. T. Nakamura, T. Miyamato and Y. Yamada, Complex Permeability Spectra of Polycrystalline Li-Zn Ferrite and Application to EM-Wave Absorber, J. Magn. Magn. Mater., **256**, 340 (2003).
4. A. Lakshman, K.H. Rao and R.G. Mendiratta, Magnetic properties of In^{3+} and Cr^{3+} substituted Mg-Mn ferrites, J. Magn. Magn. Mater., **250**, 92 (2002).
5. N. Rezlescu, L. Rezlescu, P.D. Popa and E. Rezlescu, Inf[illegible] Additives on the Properties of a Ni–Zn Fe[illegible]e with low Curie Point, J. Magn. Magn. Mater., **19[illegible]** 215-216 (2000).
6. H.[illegible] Zaki and S.F. Mansour, The Influence of Ge[illegible]and Ti^{4+} Ions Substitution on the Magnetic Properties of Copper Ferrite, Mater. Chem. Phys., **88**, 326 (2004).
7. E. Rezlescu, L. Sachelarie, P.D. Popa and N. Reslescu, Effect of Substitution of Divalent Ions on the Electrical and Magnetic Properties of Ni-Zn-Me Ferrites, IEEE Trans. Magn., **36(6)**, 3962-3967 (2000).
8. M.M. Haque, M. Huq and M.A. Hakim, Densification, Magnetic and Dielectric Behaviour of Cu-Substituted Mg–Zn Ferrites, Materials Chemistry and Physics, **112(2)**, 580-586 (2008).
9. S.H. Seo and J.H. Oh, Effect of MoO_3 Addition on Sintering Behaviors and Magnetic Properties of Nicuzn Ferrite for Multilayer Chip Inductor, IEEE Trans. Magn., **35(5)**, 3412-3414 (1999).

10. M.M. Haque, M. Huq and M.A. Hakim, Influence of CuO and Sintering Temperature on the Microstructure and Magnetic Properties of Mg–Cu–Zn Ferrites, J. Magn. Magn. Mater., 2008; **320(21)**, 2792–2799 (2008).
11. J. Bera and P.K. Roy, Effect of Grain Size on Electromagnetic Properties of $Ni_{0.7}Zn_{0.3}Fe_2O_4$ Ferrite, Physics B., **363,** 128 (2005).
12. K.S. Amarendra, T.C. Goel and R.G. Mendiratta, Magnetic Properties of Mn-Substituted Ni–Zn Ferrites, J. Appl. Phys., **92(7),** 3872 (2002).
13. A.A. Sattar, H.M.E. Sayed, K.M.E. Shokrofy and M.M.E. Tabey, Improvement of the Magnetic Properties of Mn-Ni-Zn Ferrites by the Non-Magnetic Al^{3+} Ion Substitution, J. Appl. Sci., **5(1)**, 162 (2005), .
14. G.T. Rado, Magnetic Spectra of Ferrites, Rev. Mod. Phys., **25**, 81 (1953).
15. J. Smit and H.M.J. Wijn, Ferrites (The Netherland: Philips Technical Library Eindhoven), (1959).
16. E. Scloemann, Microwave Behavior of Partially Magnetized Ferrites, J. Appl. Phys., **41**, 204 (1970).
17 J.P. Bouchaud and P.G. Zerah, The Initial Susceptibility of Ferrites: A Quantitative Theory, J. Appl. Phys., **67**, 5512 (1990).
18. J.B. Nelson and D.P. Riley, An Experimental Investigation of Extrapolation Methods in the Derivation of Accurate Unit-Cell Dimensions of Crystals, Proceeding of Physical Society, **57(3)**, 160 (1945).
19. S. Karimunnesa, D,P. Paul, S. Akter, S. Akhter, D.K. Saha and H.N. Das, Investigations on The Structural, Magnetic and Electrical Properties of $Li_{0.5-X/2}CdxBi0_{.02}Fe_{2.48-X/2}O_4$ Ferrites with the Variation of Cd Bang, J. Phys., **13**, 109 (2013).
20. L. Vegard, Die Constitution Der Mischkristalle Und Die Raumfüllung Der Atome, Physics and Astronomy, **5**, 17 (1921).
21. O.M. Hemeda and M.M. Barkat, Effect of Hopping Rate and Jump Length of Hopping Electrons on the Conductivity and Dielectric Properties of Co–Cd Ferrite, J. Magn. Mang. Mater., **223**, 127 (2001).
22. B.P. Ladgaonkar, P.N. Vasambekar and A.S. Vaingankar, Effect of Zn^{2+} and Nd^{3+} Substitution on Magnetisation and AC Susceptibility of Mg Ferrite, J. Magn. Magn. Mater., **210(1-3)**, 289 (2000).
23. S.S. Bellad, S.C. Watawe and B.K. Chougule, Microstructure and Permeability Studies of Mixed Li-Cd Ferrites, J. Magn. Magn. Mater.,**195(1)**, 57 (1999).
24. F.C. Romejin, Physical and Crystallographic Properties of Some Spinel, Philips Res. Rept., **8**, 304 (1953).
25. E. Kato, Phase Transition of Li_2O-Fe_2O_3 System. II. Thermal and Electric Properties of Lithium Ferrospinel $LiFe_5O_8$. Bull, Chem. Soe. Japn., **31(1)**, 113 (1958).
26. D. Ravinder and P.J.V.B. Reddy, Thermoelectric Power Studies of Polycrystalline Magnesium Substituted Lithium Ferrites, J. Magn. Magn. Mater., **263**, 127 (2003).
27. A. Globus, Cardiff Conference, USA (1975).
28. S.S. Bellad and B.K. Chougule, Microstructure-Dependent Magnetic Properties of Li-Cd Ferrites, Mater. Res. Bull., **33**, 1165 (1998).
29. A.M. Shaike, S.C. Watawe, S.S. Bellad, S.A. Jadhav and B.K. Chougule, Microstructural and Magnetic Properties of Zn Substituted Li–Mg Ferrites, Mater. Chem. and Phys., **65**, 46 (2000).
30. T. Nakamura, T. Miyamoto and Y. Yamada, Complex Permeability Spectra of Polycrystalline Li–Zn Ferrite and Application to EM-Wave Absorber, J. Magn. Magn. Mater., **256,** 340 (2003).
31. J.L. Snoek, Dispersion and Absorption in Magnetic Ferrites at Frequencies Above One Mc/S, Physica, **14**, 207-217 (1948).
32. S.T. Mahamud, A.K.M.A. Hossain, A.K.M.A. Hakim, M. Seki, T. Kawai and H. Tabata, Influence of Microstructure on The Complex Permeability of Spinel Type Ni-Zn Ferrites, J. Magn. Magn. Mater., **305**, 269 (2006).
33. K.J. Overshott, The Causes of the Anomalous Loss in Amorphous Ribbon Materials, IEEE Trans. Magn., **17**, 2698 (1981).
34. F.G. Brockman, P.H. Dowling and W.G. Steneck, Dimensional Effects Resulting From a High Dielectric Constant Found in a Ferromagnetic Ferrite, Phys. Rev., **77**, 85 (1950).